

N O T I C E

THIS DOCUMENT HAS BEEN REPRODUCED FROM
MICROFICHE. ALTHOUGH IT IS RECOGNIZED THAT
CERTAIN PORTIONS ARE ILLEGIBLE, IT IS BEING RELEASED
IN THE INTEREST OF MAKING AVAILABLE AS MUCH
INFORMATION AS POSSIBLE

NASA Technical Memorandum 82597

(NASA-TM-82597) REDUCED ANNEALING
TEMPERATURES IN SILICON SOLAR CELLS (NASA)
10 p HC A02/MF A01 CSCL 10A

N81-23627

Unclas

G3/44 42404

Reduced Annealing Temperatures in Silicon Solar Cells

I. Weinberg and C. K. Swartz
Lewis Research Center
Cleveland, Ohio



Prepared for the
Fifteenth Photovoltaic Specialists Conference
sponsored by the Institute of Electrical and Electronics Engineers
Kissimmee, Florida, May 12-15, 1981

NASA

REDUCED ANNEALING TEMPERATURES IN SILICON SOLAR CELLS

I. Weinberg and C. K. Swartz

National Aeronautics and Space Administration
Lewis Research Center
Cleveland, Ohio 44135

ABSTRACT

Silicon solar cells processed by ion-implantation from float zone, 0.1 ohm-cm boron-doped silicon with reduced oxygen and carbon content show greatly reduced, fluence-dependent annealing temperatures after irradiation by 1-MeV electrons. Cells irradiated to a fluence of $5 \times 10^{13}/\text{cm}^2$ showed recovery to 96 percent of the pre-irradiation short circuit current on annealing at 200° C, with complete annealing occurring at 275° C. Cells irradiated to $10^{14}/\text{cm}^2$, showed a reduction in annealing temperature from the usual 500° to 300° C. Annealing kinetic studies yield an activation energy of (1.5 ± 0.2) eV for the low fluence, low temperature anneal. Comparison with activation energies previously obtained from IR and EPR indicate that the presently obtained activation energy is consistent with the presence of either the divacancy or the carbon interstitial carbon substitutional pair, a result which agrees with our conclusion based on defect behavior in boron-doped silicon. It is concluded that reduction in annealing temperature below 200° C may possibly be achieved by further lowering the concentration of carbon in the unirradiated silicon and/or reducing the divacancy concentration after irradiation.

I. INTRODUCTION

Theoretical calculations predict that 0.1 ohm cm n^+p silicon solar cells can attain AMO efficiencies as high as 18 percent (1,2). However, when compared to the higher resistivity cells currently used in space, these low resistivity cells experience greater radiation induced degradation and require annealing temperatures of approximately 500° C to restore cell performance. This temperature is somewhat higher than the 400° C temperature required to anneal the current space cells (3). One possible solution to the degradation problem lies in attaining the capability to periodically anneal and thus restore cell performance in space. However, at such high temperatures, irreversible damage to array components occurs. On the other hand temperatures of 200° C or lower are acceptable provided welded rather than soldered interconnects are used (4).

Motivated by the requirement for lower annealing temperatures we have been conducting a program aimed at achieving a reduction in the temperature required to anneal 0.1 ohm-cm cells. Our initial steps in this program consisted of previ-

ously published calculations which showed that removal of a defect believed to contain oxygen should result in a sizeable reduction in the required annealing temperature (5). In addition, other major defects containing oxygen and carbon have been identified as being important in radiation damage to p-type silicon (6). Thus in order to explore the possibility of attaining reduced annealing temperatures in silicon solar cells we have determined the annealing characteristics of radiation damaged solar cells fabricated by ion-implantation from silicon containing reduced concentrations of carbon and oxygen. Ion-implantation was chosen as the fabrication technique because it is a relatively clean process which introduces less oxygen when compared to the standard diffusion techniques currently in use.

II. EXPERIMENTAL PROCEDURES

The solar cells were fabricated from vacuum float zone, boron-doped, 0.1 ohm-cm silicon whose oxygen and carbon contents were $< 5 \times 10^{15}/\text{cm}^3$. The cell junctions were formed by ion-implantation of 10 KeV phosphorus ions followed by a multistep furnace anneal in nitrogen (7). During the furnace anneal, the cells were held at 550° C for 15 minutes and the reannealed at 850° C for 2 hours. Data obtained using these cells was compared with our previous annealing data on 0.1 ohm-cm cells (3). These latter cells were fabricated from vacuum float zone silicon containing $10^{16}/\text{cm}^3$ oxygen and carbon. Junction fabrication was by diffusion of phosphorus oxytrichloride at 950° C for 60 minutes (3). All cells were processed without anti-reflection coating, cover glass or back surface field. Irradiation was by 1 MeV electrons at fluences ranging from 5×10^{13} to $10^{15}/\text{cm}^2$. After irradiation, the cells were isochronally and isothermally annealed in helium. During the isochronal anneal, temperature was varied in 50° C steps with time at temperature being 20 minutes. Air mass zero performance parameters were determined before and after irradiation and at each step in the anneal using a xenon-arc solar simulator. Diffusion lengths for annealing kinetic studies were determined by an X-ray excitation technique (8).

III. EXPERIMENTAL RESULTS

Figure 1 shows isochronal annealing data for the diffused junction cells from our previous work

(3). It is seen from the figure that annealing temperatures around 500° C, independent of fluence, are required to recover performance of these cells. Isochronal annealing data for the present ion-implanted cells are shown in figure 2, where it is clearly seen that the recovery temperature is fluence dependent with complete recovery occurring at 300° C for fluences, $\phi < 10^{14}/\text{cm}^2$. At higher fluence, reverse annealing is observed at $T > 400^\circ \text{C}$, and the recovery temperature approaches 500° C.

For the high purity, ion-implanted cells, isothermal annealing studies show that substantial recovery occurs below 300° C. Figure 3 shows partial recovery below this temperature for $\phi = 10^{14}/\text{cm}^2$. However, at $\phi = 5 \times 10^{13}/\text{cm}^2$ (equivalent to approximately 1 year in Geosynchronous orbit) substantial annealing occurs (figs. 4 and 5). From figure 4 it is seen that, at 275° C for this reduced fluence, recovery is almost complete at 2 hours. At 250° C significant recovery occurs after 5 hours. Because longer times are required for lowered annealing temperatures one would expect that any annealing which occurred at 200° C would require longer annealing times. That such is the case is seen in figure 5 where substantial recovery occurs, for $T = 200^\circ \text{C}$, at 46 hours. To the best of our knowledge this is the lowest temperature for which significant annealing has occurred in n^+p silicon solar cells.

IV. DISCUSSION

The major feature of the present data is the greatly reduced, fluence-dependent annealing temperature observed for the high purity silicon processed by ion-implantation. Since annealing is a process which reduces the concentration of radiation induced defects, it is appropriate to attempt an identification of the defects which are present in the silicon at the lower fluences and which are reduced in number by the low temperature anneal. To facilitate such identification, it is advantageous to examine defect behavior utilizing a technique such as Deep Level Transient Spectroscopy (DLTS). However, because the sensitivity of DLTS decreases with decreased resistivity the technique lacks sufficient sensitivity, especially at the lower fluences, for 0.1 ohm-cm cells. Thus detailed data of defect energy levels and concentrations are unavailable for these low resistivity cells. In lieu of this, our approach is to use existing data concerning the radiation induced defects in boron-doped silicon and to combine these with information obtained from the present data by a study of annealing kinetics. Hopefully such an approach will supply insight into the defect or defects which should either be eliminated or passivated to achieve annealing at even lower temperatures than those found in the present work.

Radiation Induced Defects in Boron-Doped Silicon

Figure 6 shows the relative defect concentration and energy levels for 0.3 ohm-cm, boron-doped silicon obtained during an isochronal anneal (6). This is the lowest resistivity for which we were able to find DLTS data in the literature. It is believed to be sufficiently close in resistivity

to the present 0.1 ohm-cm material to be a useful guide in further analysis. Additional information is given in table I where it can be seen that ambiguity exists in several cases and that the atomic configurations of several of the defects are unavailable. However, the pertinent information for the present case is the fact that there are only two possible defects which anneal at 300° C. The defects in question are the divacancy at $E_v + 0.23 \text{ eV}$ and the carbon-carbon pair at $E_v + 0.38 \text{ eV}$. Hence, from the data presented in table I, it is reasonable to suspect that the defect or defects which are removed by the low temperature ($T < 300^\circ \text{C}$) annealing are the divacancy and possibly the carbon-carbon pair. With respect to the fluence dependence of the annealing temperatures, we assume that the production rate of the additional defects in figure 6 is fluence dependent, such that their production rate is low below $\phi < 10^{14}/\text{cm}^2$. However, we have no experimental evidence to support this assumption.

Annealing Kinetics

The activation energy for annealing is obtained from the relation (14).

$$K = K_0 \exp \left(\frac{-E_A}{k_B T} \right) \quad (1)$$

where K is the rate constant, E_A is the activation energy, T is the temperature and K_0 is a constant which is frequently taken to be on the order of the maximum vibrational frequency of the lattice. If the annealing follows first order kinetics then:

$$N = N_0 \exp Kt \quad (2)$$

and if second order:

$$\frac{N}{N_0} = \frac{1}{1 + KN_0 t} \quad (3)$$

where N is the defect concentration at time t and N_0 the defect concentration at the beginning of the reaction (annealing). In lieu of concentrations, we use diffusion lengths, a quantity which we routinely measure during annealing. Assuming the presence of one dominant defect, it follows that (15)

$$\frac{1}{L^2} - \frac{1}{L_0^2} = BN \quad (4)$$

where L_0 is the preirradiation diffusion length, L is the diffusion length at time t during the anneal, and B is a constant at constant temperature. Combining equations (2), (3), and (4), we obtain for first order kinetics

$$\frac{1}{L^2} - \frac{1}{L_0^2} = C_1 \exp Kt \quad (5)$$

and for second order kinetics

$$\left(\frac{1}{L^2} - \frac{1}{L_0^2}\right)^{-1} = C_2 + \frac{Kt}{B} \quad (6)$$

where C_1 and C_2 are constants

Plots of equation 6 for $\phi = 5 \times 10^{13}/\text{cm}^2$ are shown in figures 7 and 8 where it is seen that the annealing data give a good fit to second order kinetics. On the other hand data plots of equation (5) show that first order kinetics do not apply in the present case. From the slopes of the straight lines in figures 7 and 8, one obtains the quantity K/B . Because equation (1) can be written as:

$$\frac{K}{B} = \frac{K_0}{B} \exp\left(\frac{-E_A}{k_B T}\right) \quad (7)$$

a similar plot of K/B vs $1/T$ should yield a straight line from which E_A can be determined. The required plot is shown in figure 9, from which,

$$E_A = (1.5 \pm 0.2) \text{ eV}$$

The activation energy for divacancy annealing, from infra-red studies (16) is 1.2 eV while that obtained from EPR (12) is 1.3 eV. For the carbon-carbon pair, the activation energy for defect re-orientation, is 1.2 eV from EPR studies (10). No activation energy for annealing is available for the carbon-carbon pair. However, the activation energy for atomic re-orientation has, in the case of the divacancy, been found equal to that for annealing (16). If we assume this to be the case for the carbon-carbon pair then the activation energy obtained from the current annealing kinetic studies is consistent with the presence of either the divacancy or the carbon pair below 300°C at the lower fluence. The annealing process below 300°C is thus one in which either or both of these defects is annihilated, with temperatures above 200°C being necessary to remove the defect.

We conclude from the annealing kinetics study that either the divacancy or carbon pair defect is present at the lower fluences. This agrees with our conclusion based on defect identification studies. The present work therefore suggests that at the lower fluences annealing below 200°C could be achieved with additional lowering of the divacancy and/or carbon concentration.

Conclusions

From the data and analysis presented here, the following conclusions are reached:

Processing cell junctions by ion-implantation from 0.1 ohm-cm, float zone boron-doped silicon with reduced oxygen and carbon content ($\leq 5 \times 10^{15}/\text{cm}^3$) drastically reduces the temperature required to remove degradation in n^+p silicon solar cells after irradiation by 1 MeV electrons.

The annealing kinetics are fluence dependent, i.e., for a 1 MeV electron fluence of $5 \times 10^{13}/\text{cm}^2$, recovery to 96 percent of preirradiation values occurs at 200°C , while for a fluence of $10^{14}/\text{cm}^2$ complete annealing occurs at 300°C . Above $10^{14}/\text{cm}^2$, the annealing recovery temperature

increases and approaches the normally expected 500°C at $\phi = 10^{15}/\text{cm}^2$.

The annealing kinetics are second order, the activation energy for annealing being $(1.5 \pm 0.2 \text{ eV})$. Comparison with data obtained from EPR and infrared studies indicates that this activation energy is consistent with the presence of either the divacancy or carbon interstitial-carbon substitutional pair. This result agrees with our conclusions based on available data regarding defect behavior in p-type silicon.

Reduction in annealing temperature below 200°C appears possible by lowering the concentration of the carbon in the starting silicon and/or lowering the concentration of divacancies after irradiation.

REFERENCES

1. H. W. Brandhorst, Jr., "Silicon Solar Cell Efficiency - Practice and Promise," in Proceedings of the 9th Photovoltaic Specialists Conference, New York: Institute of Electrical and Electronics Engineers, Inc., 1972, pp. 37-43.
2. M. P. Godlewski, H. W. Brandhorst, Jr., and C. R. Baraona, "Effects of High Doping Levels on Silicon Solar Cell Performance," in Proceedings of the 11th Photovoltaic Specialists Conference, New York: Institute of Electrical and Electronics Engineers, Inc., 1975, pp. 32-35.
3. I. Weinberg and C. K. Swartz, "Annealing of Radiation Damage in 0.1 and 2 ohm-cm Silicon Solar Cells," NASA TP-1559, 1979.
4. R. Buhs, H. J. Duerre, and H. W. Boller, "Welding of Solar Cells in Production Line," in Proceedings of the 11th Photovoltaic Specialists Conference, New York: Institute of Electrical and Electronics Engineers, Inc., 1975, pp. 126-133.
5. I. Weinberg and C. K. Swartz, "Origin of Reverse Annealing in Radiation-Damaged Silicon Solar Cells," Appl. Phys. Lett., vol. 36, no. 8, pp. 693-695, 1980.
6. P. M. Mooney, L. T. Cheng, M. Süli, J. D. Gerson, and J. W. Corbett, "Defect Energy Levels in Boron-Doped Silicon Irradiated with 1-MeV Electrons," Phys. Rev. B, vol. 15, no. 8, pp. 3836-3843, 1977.
7. The Ion-Implanted Cells were fabricated by the Spire Corporation - Bedford, Mass.
8. W. Rosenzweig, "Diffusion Length Measurements by Means of Ionizing Radiation," Bell Sys. Tech. J., vol. 41, no. 5, pp. 1573-1588, 1962.
9. Y. H. Lee, J. W. Corbett, and K. L. Brower, "EPR of a Carbon-Oxygen-Divacancy Complex in Irradiated Silicon," Phys. Stat. Sol., vol. (a)41, pp. 637-647, 1977.
10. K. L. Brower, "EPR of a Jahn-Teller Distorted 111 Carbon Interstitially in Irradiated Silicon," Phys. Rev. vol. B9, pp. 2607-2617, 1974.
11. L. C. Kimerling, "Defect States in Electron Bombarded Silicon: Capacitance Transient Analyses," Radiation Effects in Semiconductors, Conference Series No. 31, London: Institute of Physics, 1977, pp. 221-230.

12. G. D. Watkins and J. W. Corbett, "Defects in Irradiated Silicon: Electron Paramagnetic Resonance of the Divacancy," Phys. Rev. vol. 138, no. 2A, pp. 543-555, 1965.
13. K. L. Brower, "EPR of a VOI Si Interstitial Complex in Irradiated Silicon," Phys. Rev. vol. B14, no. 3, pp. 872-883, 1976.
14. J. W. Corbett, Electron Radiation Damage in Semiconductors and Metals, New York: Academic Press, pp. 36-43, 1966.
15. W. Shockley and W. T. Read, Jr., "Statistics of the Recombination of Holes and Electrons," Phys. Rev. vol. 87, pp. 835-841, 1952.
16. L. J. Cheng, J. C. Corelli, J. W. Corbett, and G. D. Watkins, "1.8-, 3.3-, and 3.9- μ Bands in Irradiated Silicon: Correlations with the Divacancy," Phys. Rev., vol. 152, no. 2, pp. 761-774, 1966.

TABLE I - ANNEALING TEMPERATURES OF MAJOR
DEFECTS IN BORON-DOPED SILICON

Energy level, eV	Defect	Annealing temperature, °C		Detection method
		In	Out	
$E_V + 0.38$	V-O-C or C_I-C_S	<30	400	EPR ⁹ , DLTS ⁶
		<30	300	EPR ¹⁰ , DLTS ¹¹
$E_V + 0.23$	Divacancy	<30	300	EPR ¹² , DLTS ^{6,11}
$E_C - 0.27$	B_I-O_I or B_I-B_S	<30	200	DLTS ⁶
		<30	180	DLTS ¹¹
$E_V + 0.30$	B-O-V or S_I-S_I	100	400+	DLTS ⁶
		200	500	EPR ¹³ , DLTS ¹¹
$E_V + 0.26$	-----	270	400	DLTS ⁶
$E_V + 0.43$	-----	<30	200	DLTS ⁶

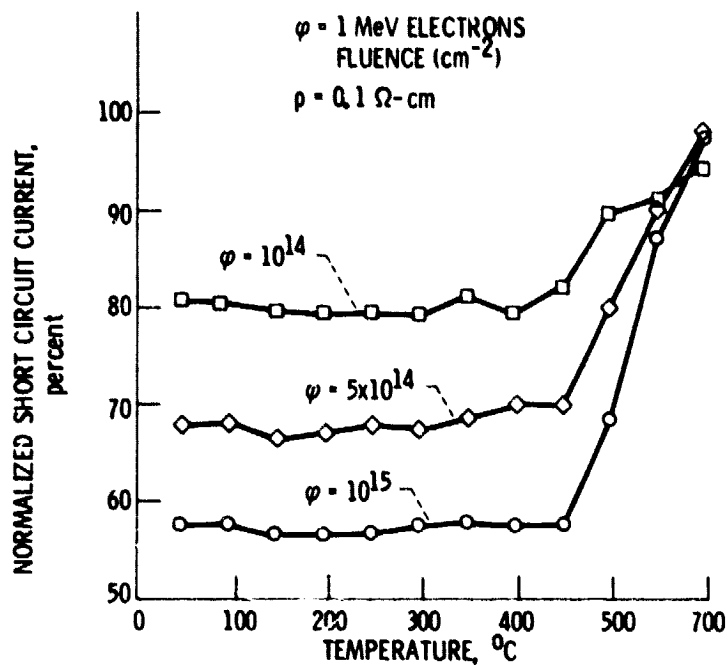


Figure 1. - Isochronal anneal of diffused junction cells.
(High O and C silicon)

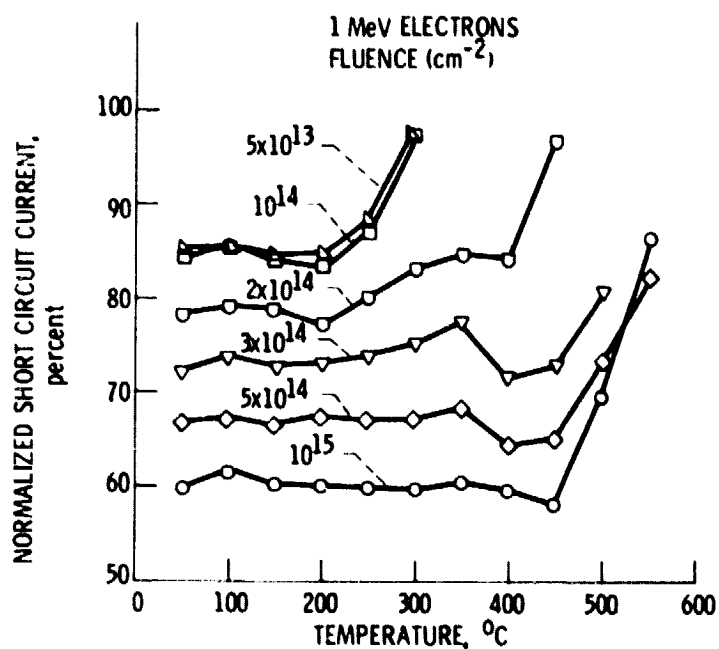


Figure 2. - Isochronal anneal of ion-implanted $0.1 \Omega\text{-cm}$ cells. (Low O and C silicon)

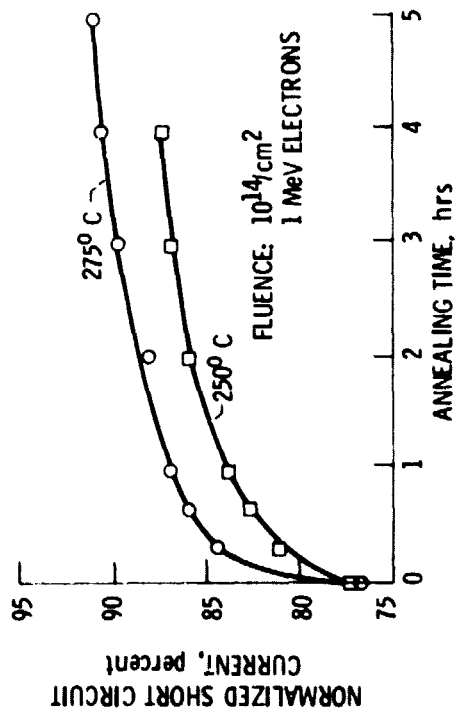


Figure 3. - Isothermal annealing of 0.1 Ω -cm cells.

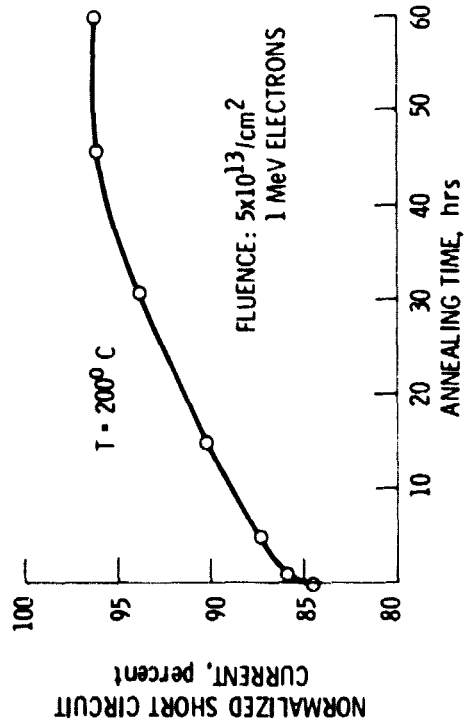


Figure 5. - Isothermal annealing at 200° C of 0.1 Ω -cm ion-implanted cell.

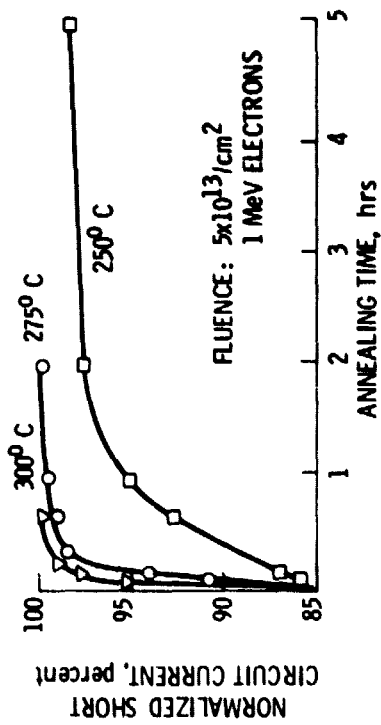


Figure 4. - Isothermal annealing of ion-implanted 0.1 Ω -cm cells.

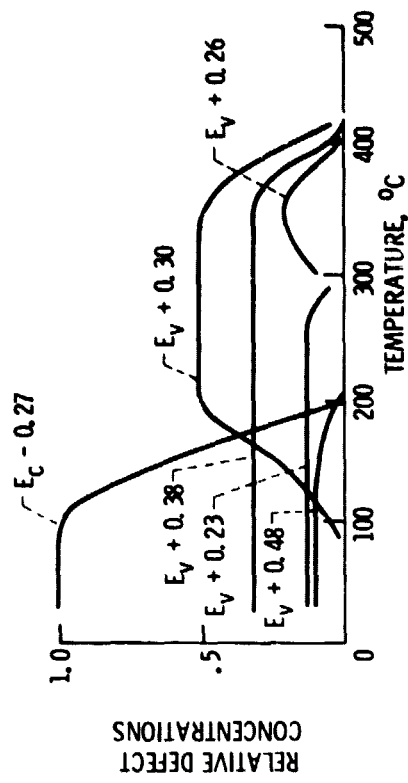


Figure 6. - DLTS data for 0.3 Ω -cm P - Si isochronally annealed after 1 - MeV electron irradiation (after ref. 6).

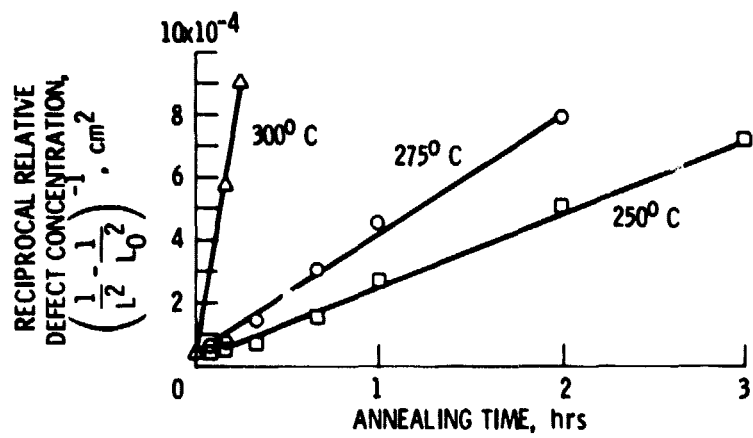


Figure 7. - Second order kinetics plot: $\phi = 5 \times 10^{13} \text{ cm}^2$, 1 MeV electrons.

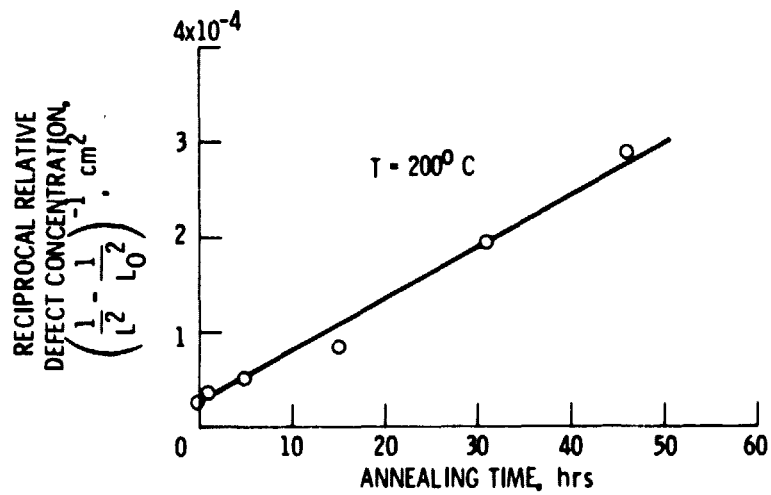


Figure 8. - Second order kinetics plot, $\phi = 5 \times 10^{13} \text{ cm}^2$, 1 MeV electrons.

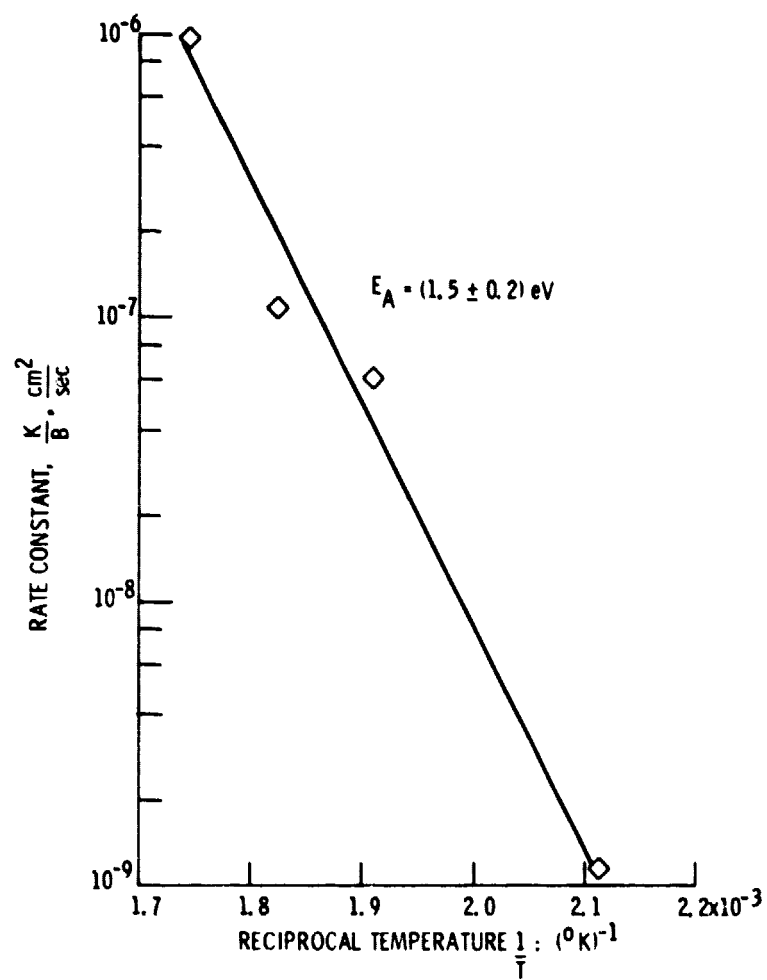


Figure 9. - Plot used to obtain migration energies $\phi = 5 \times 10^{13} \text{ cm}^{-2}$
1 MeV electrons.